

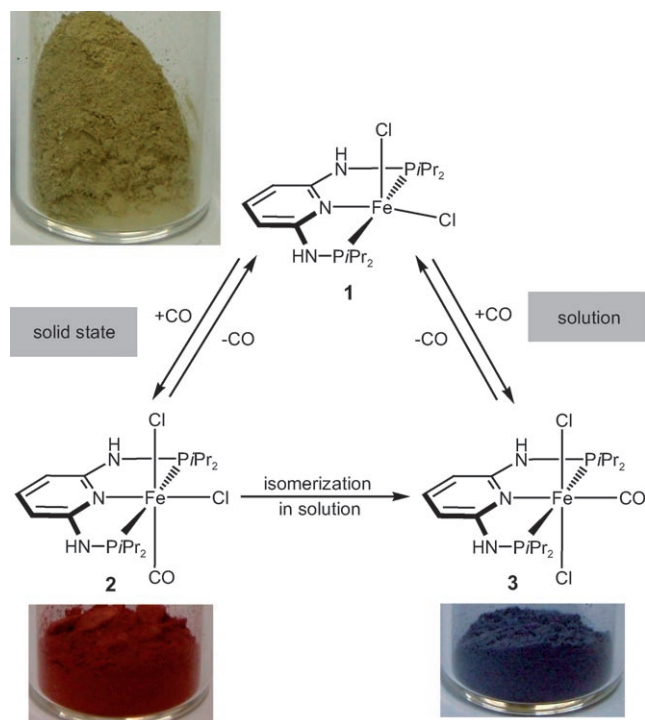
Stereospecific and Reversible CO Binding at Iron Pincer Complexes**

David Benito-Garagorri, Michael Puchberger, Kurt Mereiter, and Karl Kirchner*

The design of molecular components capable of self-assembling in the solid state to form well-defined and functional superstructures is an important goal in materials science.^[1] Self-assembly induced by weak noncovalent forces, particularly hydrogen bonds, has proven especially effective, largely because of the design of tailored recognition elements in the form of hydrogen-bond donor-acceptor arrays that direct the assembly process.^[2,3] Furthermore, chemical transformations that occur in self-assembled structures have received increased attention owing to their applicability as molecular switches or sensors.^[4] However, such reactions are rare, because chemical reactions at the molecular level are likely to destroy the architecture and properties of the crystal lattice. Therefore, the best-explored reactions in closed structures are transformations in which the overall atom content of the system remains unchanged, for example, reversible photochemical isomerization processes.^[5] A remarkable example of a solid-state reaction in which, despite a change in the overall atom content, crystallinity is maintained, is the reversible binding of gaseous SO₂ to square-planar platinum(II) pincer complexes.^[6]

We recently reported the synthesis of the coordinatively unsaturated iron PNP pincer complex [Fe(PNP-*i*Pr)Cl₂] (**1**, Scheme 1; PNP-*i*Pr = *N,N'*-bis(diisopropylphosphino)-2,6-diaminopyridine).^[7–9] This complex features metal-bound chloride ions as hydrogen-bond acceptors and secondary amino groups on the pincer ligand as hydrogen donors. As determined by X-ray crystallography,^[10] **1** self-assembles in the solid state through intermolecular Fe–Cl...H–N hydrogen bonds to form a distorted diamond-type three-dimensional network with incorporated solvent (THF; Figure 1).

The THF molecules are located in continuous channels with oval cross sections extending parallel to the *a* axis of the [Fe(PNP-*i*Pr)Cl₂] network. When exposed to 1 atm of gaseous



Scheme 1. Stereospecific formation of *cis*- and *trans*-[Fe(PNP-*i*Pr)(CO)(Cl)₂] (**2** and **3**).

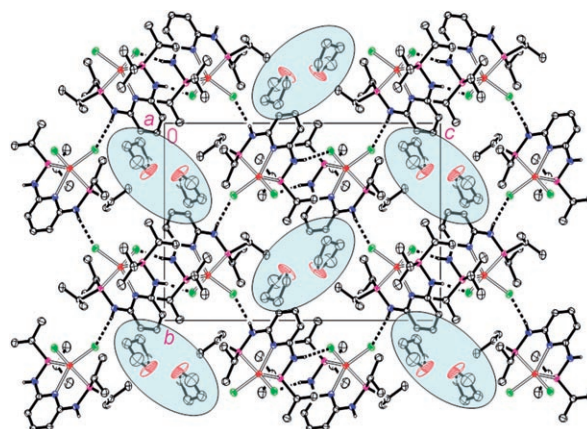


Figure 1. Packing diagram of **1**·THF at *T* = 100 K in a view down the *a* axis. Fe–Cl...H–N hydrogen bonds are depicted as dashed lines; THF molecules are highlighted in ovals.

CO at room temperature, solid **1** is rapidly converted into solid *cis*-[Fe(PNP-*i*Pr)(CO)(Cl)₂] (**2**) as the sole product, as indicated by a color change in the material from light yellow to deep red (Scheme 1). However, when single crystals in the form of **1**·THF were exposed to CO, the formation of **2** takes

[*] Dr. D. Benito-Garagorri, Prof. Dr. K. Kirchner
Institute of Applied Synthetic Chemistry
Vienna University of Technology
Getreidemarkt 9, 1060 Vienna (Austria)
Fax: (+43) 1-58801-16399
E-mail: kkirch@mail.zserv.tuwien.ac.at

Dr. M. Puchberger
Institute of Materials Chemistry
Vienna University of Technology
Getreidemarkt 9, 1060 Vienna (Austria)

Prof. Dr. K. Mereiter
Institute of Chemical Technologies and Analytics
Vienna University of Technology
Getreidemarkt 9, 1060 Vienna (Austria)

[**] Financial support by the Austrian Science Foundation (FWF) is gratefully acknowledged (Project No. P16600-N11).

Supporting information for this article is available on the WWW under <http://dx.doi.org/10.1002/anie.200803665>.

place more slowly. X-ray powder diffraction studies revealed that **1**·THF gradually loses THF to give a desolvated form of **1**, which is then completely converted to **2** within approximately 2 min after exposure to 1 atm CO at ambient temperature. It therefore seems reasonable to assume that desolvation of **1**·THF takes place with at least partial preservation of the network structure, with the sites formerly occupied by solvent molecules now serving as channels through which CO can readily diffuse into the solid.^[11] Unequivocal evidence for the crystalline nature of complexes **1** and **2** has been obtained by X-ray powder diffraction.

CO binding is fully reversible, and heating solid samples of either **2** or **3** at 100 °C for 5 min under vacuum leads to the complete regeneration of analytically pure crystalline **1**, which can again be treated with CO either in the solid state or in solution to give **2** or **3**. At room temperature loss of CO is slow, needing about two weeks to completely regenerate **1**. This “on” and “off” process can be repeated for at least five cycles without any noticeable decomposition of **1**. The reversibility of this reaction in the solid state has been elucidated by time-resolved IR spectroscopy, where the stretching vibration of coordinated CO in **2** ($\nu_{\text{CO}} = 1947 \text{ cm}^{-1}$) was monitored. The reaction of **1** with CO, carried out at 25 °C, was complete in about 2 min (Figure 2). The

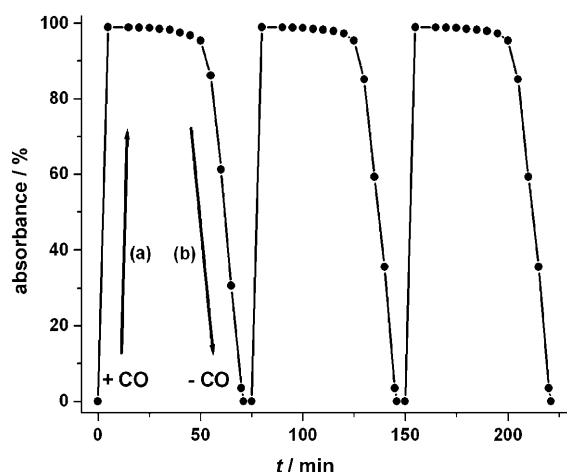


Figure 2. Time dependence of the intensity of the stretching frequency ν_{CO} of **2** ($\bar{\nu} = 1947 \text{ cm}^{-1}$): a) increase during the reaction of **1** and CO at 25 °C and 1 atm CO; b) decrease upon heating from 25 to 200 °C in air.

desorption of CO was performed within approximately 70 min by raising the temperature from 25 to 200 °C with a heating rate of 2.5 °C min^{-1} (Figure 2). Moreover, thermogravimetric analyses of **2** and **3** show weight losses corresponding to the release of one equivalent of CO and regeneration of **1**.

On the other hand, when CO was bubbled into an acetone solution of **1** for 2 min, a blue solid was formed, which was identified as *trans*-[Fe(PNP-*i*Pr)(CO)(Cl)₂] (**3**; Scheme 1). The structural features of **3**·(CH₃)₂CO were determined by single crystal X-ray analysis (Figure 3).

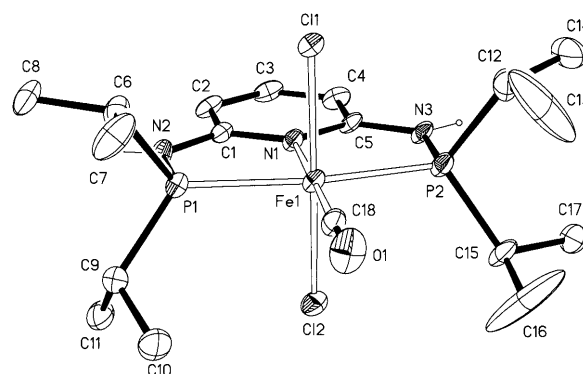


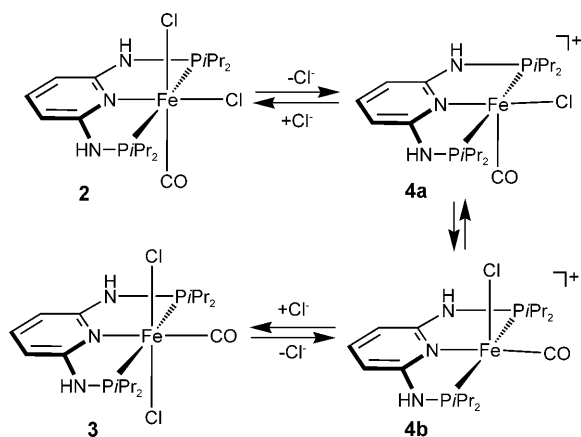
Figure 3. ORTEP depiction of the crystal structure of **3**·(CH₃)₂CO. Thermal ellipsoids are set at the 50% probability level; solvent molecules and most H atoms are omitted for clarity. Selected bond lengths [Å] and angles [°]: Fe1–Cl1 2.344(1), Fe1–Cl2 2.345(1), Fe(1)–P(1) 2.250(1), Fe1–P2 2.252(1), Fe1–N1 1.989(3), Fe1–C18 1.758(4); N1–Fe1–C18 179.4(2), P1–Fe1–P2 168.11(5).

Accordingly, the reaction of **1** with CO proceeds stereospecifically yielding either *cis*- or *trans*-[Fe(PNP-*i*Pr)(CO)(Cl)₂] depending on the reaction conditions employed. Both transformations are accompanied by changes in the color of the products, the coordination geometry around the iron center, and the spin states. It should be noted that the reaction of **1** with CO is extremely selective, since this complex does not react with other gases such as NO or SO₂.

Complex **1** is paramagnetic with an effective magnetic moment $\mu_{\text{eff}} = 5.2 \mu_{\text{B}}$, indicating the presence of four unpaired electrons and a quintet ground state ($S = 2$), whereas complexes **2** and **3** are diamagnetic ($S = 0$).

The exclusive formation of **2** in the solid state and of **3** in solution was confirmed by solid-state NMR spectroscopy. In the solid state the two complexes give rise to signals at $\delta = 111.5$ and 125.3 ppm in the $^{31}\text{P}\{^1\text{H}\}$ NMR spectrum, respectively. In the ^{15}N NMR spectra, the pyridine nitrogen atom in **2** appears at $\delta = 119.7 \text{ ppm}$ as a result of the *cis* conformation of the chloride ions, while in **3**, where the chloride ions are in a *trans* arrangement, it gives rise to a signal at $\delta = 167.5 \text{ ppm}$.

In DMSO at room temperature, the red *cis* isomer **2** transforms rapidly (within ca. 90 min) into the blue *trans* complex **3**. The isomerization mechanism most likely involves chloride dissociation and the formation of a transient cationic intermediate [Fe(PNP-*i*Pr)(CO)(Cl)]⁺ (**4**), since CO dissociation would regenerate complex **1**, and no evidence for the formation of a paramagnetic species was observed when the isomerization process was monitored by ^1H and $^{31}\text{P}\{^1\text{H}\}$ NMR spectroscopy. The pentacoordinated nature of intermediate **4** allows for the existence of two conformations, one with the CO ligand in the apical and the Cl ligand in the meridional position (**4a**) and vice versa (**4b**; Scheme 2). Subsequent coordination of a chloride ion to the second conformer yields isomer **3**, which is thermodynamically favored. This mechanism is also supported by the fact that addition of a chloride anion source (*n*Bu₄NCl) to a solution of **2** leads to longer isomerization times, whereas performing the reaction under CO atmosphere has no effect.



Scheme 2. Mechanism of the isomerization of **2** to **3** via the unsaturated intermediates **4a** and **4b**.

In summary, we have shown that the pentacoordinated iron PNP pincer complex $[\text{Fe}(\text{PNP-}i\text{Pr})\text{Cl}_2]$ (**1**) self-assembles in the solid state through intermolecular $\text{Fe}-\text{Cl}\cdots\text{H}-\text{N}$ hydrogen bonds to form a three-dimensional supramolecular network. In the solid state, this compound reacts readily with gaseous CO to stereospecifically give *cis*- $[\text{Fe}(\text{PNP-}i\text{Pr})(\text{CO})(\text{Cl})_2]$ (**2**), in which the supramolecular connectivities between single molecules appear to be maintained and for which the reaction proceeds without loss of crystallinity. In contrast, CO addition in solution affords exclusively the corresponding *trans* isomer **3**. Accordingly, this class of compounds may represent a novel type of functional materials for crystal engineering and the processing of crystalline solids.

Moreover, the selectivity and full reversibility of CO uptake and release in this material, which can be detected and monitored by a variety of techniques such as solid-state and solution NMR, UV/Vis, and IR spectroscopy as well as magnetic susceptibility measurements and X-ray powder diffraction, suggests an application potential both as an efficient CO sensor and as a crystalline switch.^[12]

Experimental Section

2: CO was passed over a solid sample of **1** (500 mg, 1.1 mmol) for 2 min, whereupon the solid changed its color from yellow to red. Yield: 530 mg (100%). Elemental analysis (%) calcd for $\text{C}_{18}\text{H}_{33}\text{Cl}_2\text{FeN}_3\text{OP}_2$: C 43.57, H 6.70, N 8.47; found: C 43.51, H 6.73, N 8.52. ^1H NMR ($[\text{D}_6]\text{DMSO}$, 20°C): δ = 8.20 (s, 2H, NH), 7.06 (t, J = 6.7 Hz, 1H, py^4), 6.01 (d, J = 6.7 Hz, 2H, $\text{py}^{3,5}$), 2.48 (m, 4H, $\text{CH}(\text{CH}_3)_2$), 1.42–1.28 ppm (m, 24H, $\text{CH}(\text{CH}_3)_2$). $^{31}\text{P}\{^1\text{H}\}$ NMR ($[\text{D}_6]\text{DMSO}$, 20°C): δ = 106.85 ppm. Solid-state NMR: ^{13}C -CP/MAS NMR (20°C): δ = 214.7 (CO), 155.9 ($\text{py}^{2,6}$), 129.9 (py^4), 92.3 ($\text{py}^{3,5}$), 19.3 ($\text{CH}(\text{CH}_3)_2$), 11.9 ppm ($\text{CH}(\text{CH}_3)_2$). ^{31}P -HPDEC (high-power decoupled) NMR (20°C): δ = 111.5 ppm. ^{15}N -CP/MAS NMR (20°C): δ = 119.7 (py), 52.6 ppm (NH). IR (ATR; attenuated total reflection): $\tilde{\nu}$ = 1947 cm^{-1} ($\nu_{\text{C-O}}$). UV/Vis (powder samples measured in diffuse reflectance): λ_{max} = 524 nm.

3: CO was bubbled into a solution of **1** (500 mg, 1.1 mmol) in acetone (10 mL) for 2 min, whereupon the color of the reaction mixture turned from yellow to blue. After removal of the solvent under reduced pressure, the remaining solid was washed twice with Et_2O (10 mL) and dried under vacuum. Yield: 503 mg (95%).

Elemental analysis (%) calcd for $\text{C}_{18}\text{H}_{33}\text{Cl}_2\text{FeN}_3\text{OP}_2$: C 43.57, H 6.70, N 8.47; found: C 43.61, H 6.65, N 8.51. ^1H NMR ($[\text{D}_6]\text{DMSO}$, 20°C): δ = 8.45 (s, 2H, NH), 7.43 (t, J = 7.2 Hz, 1H, py^4), 6.48 (d, J = 7.2 Hz, 2H, $\text{py}^{3,5}$), 2.77 (m, 4H, $\text{CH}(\text{CH}_3)_2$), 1.42–1.28 ppm (m, 24H, $\text{CH}(\text{CH}_3)_2$). $^{13}\text{C}\{^1\text{H}\}$ NMR ($[\text{D}_6]\text{DMSO}$, 20°C): δ = 224.81 (t, J = 22.7 Hz, CO), 163.1 (t, J = 9.2 Hz, $\text{py}^{2,6}$), 139.8 (py^4), 98.7 ($\text{py}^{3,5}$), 25.5 (t, J = 11.8 Hz, $\text{CH}(\text{CH}_3)_2$), 19.3 ($\text{CH}(\text{CH}_3)_2$), 18.1 ppm ($\text{CH}(\text{CH}_3)_2$). $^{31}\text{P}\{^1\text{H}\}$ NMR ($[\text{D}_6]\text{DMSO}$, 20°C): δ = 122.5 ppm. Solid-state NMR: ^{13}C -CP/MAS NMR (20°C): δ = 217.0 (CO), 155.7 ($\text{py}^{2,6}$), 132.6 (py^4), 93.9 ($\text{py}^{3,5}$), 25.2 ($\text{CH}(\text{CH}_3)_2$), 12.3 ppm ($\text{CH}(\text{CH}_3)_2$). ^{31}P -HPDEC NMR (20°C): δ = 125.3 ppm. ^{15}N -CP/MAS NMR (20°C): δ = 167.5 (py), 49.1 ppm (NH). IR (ATR): $\tilde{\nu}$ = 1956 cm^{-1} ($\nu_{\text{C-O}}$). UV/Vis (powder samples measured in diffuse reflectance): λ_{max} = 578 nm.

Received: July 27, 2008

Published online: October 20, 2008

Keywords: carbon monoxide · coordination chemistry · gas sensors · iron · pincer ligands

- [1] a) *Perspectives in Supramolecular Chemistry. The Crystal as a Supramolecular Entity* (Ed.: G. R. Desiraju), Wiley, Chichester, **1996**; b) G. R. Desiraju in *Crystal Engineering; The Design of Organic Solids*, Elsevier, Amsterdam, **1989**.
- [2] a) *Comprehensive Supramolecular Chemistry* (Eds.: J. L. Atwood, J. E. D. Davies, D. D. MacNicol, F. Vögtle), Pergamon, Oxford, **1996**; b) J.-M. Lehn, *Supramolecular Chemistry: Concepts and Perspectives*, VCH, Weinheim, **1995**; c) J.-M. Lehn, *Angew. Chem.* **1990**, *102*, 1347; *Angew. Chem. Int. Ed. Engl.* **1990**, *29*, 1304.
- [3] For examples on hydrogen-bond-mediated self-assembly, see: a) D. C. Sherrington, K. A. Taskinen, *Chem. Soc. Rev.* **2001**, *30*, 83; b) M. J. Krische, J.-M. Lehn, *Struct. Bonding (Berlin)* **2000**, *96*, 3; c) L. J. Prins, J. Huskens, F. de Jong, P. Timmerman, D. N. Reinhoudt, *Nature* **1999**, *398*, 498; d) G. Desiraju, T. Steiner in *The Weak Hydrogen Bond: Applications to Structural Chemistry and Biology*, Oxford University Press, Oxford **1999**; e) P. Brunet, M. Simard, J. D. Wuest, *J. Am. Chem. Soc.* **1997**, *119*, 2737; f) M. J. Zaworotko, *Nature* **1997**, *386*, 220; g) A. D. Burrows, C.-W. Chan, M. M. Chowdry, J. E. McGrady, D. M. P. Mingos, *Chem. Soc. Rev.* **1995**, *24*, 329; h) J. C. MacDonald, G. M. Whitesides, *Chem. Rev.* **1994**, *94*, 2383.
- [4] a) J.-M. Lehn, *Science* **2002**, *295*, 2400; b) M. D. Hollingsworth, *Science* **2002**, *295*, 2410.
- [5] a) K. Tanaka, H. Mizutani, I. Miyahara, K. Hirotsu, F. Toda, *CrystEngComm* **1999**, *1*, 8; b) J. L. Foley, L. Li, D. J. Sandman, M. J. Vela, B. M. Foxman, R. Albro, C. J. Eckhardt, *J. Am. Chem. Soc.* **1999**, *121*, 7262; c) S. Kobatake, M. Yamada, T. Yamada, M. Irie, *J. Am. Chem. Soc.* **1999**, *121*, 8450; d) A. Matsumoto, T. Odani, M. Chikada, K. Sada, M. Miyata, *J. Am. Chem. Soc.* **1999**, *121*, 11122; e) K. Novak, V. Enkelmann, G. Wegner, K. B. Wagener, *Angew. Chem.* **1993**, *105*, 1678; *Angew. Chem. Int. Ed. Engl.* **1993**, *32*, 1614; f) J. R. Scheffer, P. R. Pokkuluri in *Photochemistry in Organized & Constrained Media* (Ed.: V. Ramamurthy), VCH, New York, **1990**.
- [6] a) M. Albrecht, G. van Koten, *Adv. Mater.* **1999**, *11*, 171; b) M. Albrecht, M. Lutz, A. L. Spek, G. van Koten, *Nature* **2000**, *406*, 970; c) M. Albrecht, M. Lutz, A. M. M. Schreurs, E. T. H. Lutz, A. L. Spek, G. van Koten, *J. Chem. Soc. Dalton Trans.* **2000**, 3797.
- [7] D. Benito-Garagorri, E. Becker, J. Wiedermann, W. Lackner, M. Pollak, J. Kisala, K. Mereiter, K. Kirchner, *Organometallics* **2006**, *25*, 1900.
- [8] D. Benito-Garagorri, J. Wiedermann, M. Pollak, K. Mereiter, K. Kirchner, *Organometallics* **2007**, *26*, 217.

- [9] D. Benito-Garagorri, K. Kirchner, *Acc. Chem. Res.* **2008**, *41*, 201.
- [10] CCDC-683350, 683351, 683352 (**1**·THF at 100, 200, and 297 K) and 683353 (**3**·(CH₃)₂CO) contain the supplementary crystallographic data for this paper. These data can be obtained free of charge from The Cambridge Crystallographic Data Centre via www.ccdc.cam.ac.uk/data_request/cif.
- [11] An iron complex exhibiting a well-defined three-dimensional structure before and after solvent loss has been reported recently; see: V. Niel, A. L. Thompson, M. C. Muñoz, A. Galet, A. E. Goeta, J. A. Real, *Angew. Chem.* **2003**, *115*, 3890; *Angew. Chem. Int. Ed.* **2003**, *42*, 3760.
- [12] “Reactivity of Pincer Complexes toward Carbon Monoxide”: D. Morales-Morales in *Modern Carbonylation Methods* (Ed.: L. Kollár), Wiley, Weinheim, **2008**. For recent examples of CO sensors with metal complexes, see: a) S. Ye, W. Zhou, M. Abe, T. Nishida, L. Cui, K. Uosaki, M. Osawa, Y. Sasaki, *J. Am. Chem. Soc.* **2004**, *126*, 7434; b) A. Gulino, T. Gupta, M. Altman, S. Lo Schiavo, P. G. Mineo, I. L. Fragalà, G. Evmenenko, P. Dutta, M. E. van der Boom, *Chem. Commun.* **2008**, 2900.
-